

AUTOMOTIVE COLLISION RISK ESTIMATION UNDER COOPERATIVE SENSING

Daniel LaChapelle* Todd Humphreys* Lakshay Narula† Peter Iannucci* Ehsan Moradi-Parizi‡

*Aerospace Engineering and Engineering Mechanics, The University of Texas at Austin.

†Electrical and Computer Engineering, The University of Texas at Austin.

‡Automobile Technology Research Division, Honda R&D Americas, Inc.

ABSTRACT

This paper offers a technique for estimating collision risk for automated ground vehicles engaged in cooperative sensing. The technique allows quantification of (i) risk reduced due to cooperation, and (ii) the increased accuracy of risk assessment due to cooperation. If either is significant, cooperation can be viewed as a desirable practice for meeting the stringent risk budget of increasingly automated vehicles; if not, then cooperation—with its various drawbacks—need not be pursued. Collision risk is evaluated over an ego vehicle’s trajectory based on a dynamic probabilistic occupancy map and a loss function that maps collision-relevant state information to a cost metric. The risk evaluation framework is demonstrated using real data captured from two cooperating vehicles traversing an urban intersection.

Index Terms— sensor data fusion, automated vehicles, dynamic occupancy grid maps, collision risk assessment

1. INTRODUCTION

Recent works on automated vehicle (AV) safety target a many-fold safety advantage over human drivers [1,2]. To meet such high expectations, AVs must be designed to continuously and accurately assess their collision risk over a short time horizon. Cooperative sensing (inter-vehicle sensor data sharing and drawing sensor data from infrastructure) may significantly reduce collision risk in highly uncertain, dynamic environments [3], but its benefits have yet to be quantified. Meanwhile, serious challenges to cooperation exist: how can it be incentivized? Can the ego vehicle trust received data? How can data received be accurately placed within the ego vehicle reference frame?

This paper presents a framework for measuring the benefit of cooperation in terms of reduced collision risk and reduced risk uncertainty. Existing risk assessment schemes either assume all current and near-future traffic participants have been identified and are being tracked [4–7], or they assume a worst-case model in which blind spots are fully occupied [8]. Neither approach is well suited to an accurate measurement of risk that accounts for risk lurking in sensing blind spots with *a priori* probabilities informed by historical sensing. Moreover, existing approaches do not provide a probability distribution for assessed risk. This prevents an evaluation of risk uncertainty, and, relevant to the current paper’s aims, an evaluation of the benefit of cooperative sensing in terms of reduced risk uncertainty.

Predicting the likely evolution of a traffic situation can be performed with an object-based or an object-free representation of the environment [8]. An object-based representation assigns a class (e.g., pedestrian, cyclist, car) to each traffic participant—tracked or potential—and assumes a class-specific motion model for each [4–7]. An object-free representation does not attempt to classify other traffic participants, but only estimates current and near-future occupancy in a gridded map. To establish a proof of concept, the

current paper adopts an object-free representation, which requires only a small number of parameters to model. This can later be extended to an object-based representation for greater risk assessment accuracy [9].

Probabilistic occupancy maps (POMs, also referred to as occupancy grid maps) are a convenient object-free construct for fusing sensing data from multiple sensors, possibly from multiple cooperating agents. A POM discretizes the traffic environment into a grid [10]. To each of the grid’s cells is associated a Bernoulli random variable: the cell is occupied with probability p and empty with probability $1 - p$. Early POMs represented only static environments, whereas AV applications require dynamic maps. In either case, the state of the map at a particular epoch represents the instantaneous estimates of occupancy probabilities conditioned on all previous measurements. Methods for estimating occupancy over time from noisy measurements are known in the literature as Bayesian occupancy filters (BOFs) [11]. At each point in time, the state of the BOF is a POM. Since it was introduced for automotive motion planning [12], BOF theory has been developed in a variety of different ways [11]. Some approaches are optimized for particular sensing systems [13], whereas others reduce errors by incorporating prior map knowledge [14].

The key advantage of BOFs over traditional multi-target tracking is that BOFs sidestep the notoriously thorny combinatorial “data association problem” in which sensor measurements must be associated with a discrete observed target [15]. The BOF and related approaches do not associate sensor measurements explicitly. Instead, measurements are used to update the occupancy probability of grid cells under the assumption that the cells are statistically independent. For BOF proponents, discretization and assumed cell-to-cell statistical independence, although introducing some inaccuracy, are justified by convenience: they allow Bayesian update equations to be represented analytically and updated in parallel [16–19].

More recent dynamic mapping approaches employ particle filter tracking to ease the computational burden of BOFs. In particular, the Probability Hypothesis Density / Multi-Instance Bernoulli (PHD/MIB) filter [20] is at the core of the current paper’s risk assessment formulation. It is particularly attractive because it links the problem of dynamic state estimation of grid cells to a rigorously-founded literature in finite set statistics (FISST) [21], ensuring that particles have a well-defined physical meaning and are propagated according to Bayesian rules. A BOF approach rooted in random finite set theory enables risk estimation to incorporate not only the risk of collision with observed objects, but also with objects that have not been observed but could possibly exist, informed by historical data.

This paper makes two primary contributions. First, it develops a technique for collision risk evaluation that is amenable to data fusion from multiple cooperating vehicles (or from infrastructure), and amenable to realistic characterization of risk emerging from occluded areas (i.e., blind spots). Besides risk evaluation, the technique also offers a measure of risk uncertainty, which one would expect to

decrease under cooperative sensing. Second, the paper applies the risk assessment framework to real data captured from a pair of connected vehicles to demonstrate the benefit of cooperative sensing for a simple example scenario.

2. APPROACH

The core contribution of this paper is a framework for computing estimated collision risk based on a Bayesian occupancy filter augmented with a loss function. The BOF, along with the ego vehicle’s pose estimate, can be used to compute the probability of collision at time step k in grid cell c ; the loss function returns the severity of the collision. This paper presents accumulated risk, a quantity evaluated over a given trajectory: the accumulated risk at time step k is the cumulative sum of risks up to k .

2.1. Bayesian Occupancy Filtering

To implement a Bayesian occupancy filter, this paper adopts the PHD/MIB formalism introduced by Nuss et al. [20]. In this approach, each grid cell is modeled as an independent Bernoulli random finite set (RFS) that is either empty with probability $1 - r$ or contains a single point object with existence probability r and spatial distribution $p(\mathbf{x})$. In the two-dimensional problem, $p(\mathbf{x})$, $\mathbf{x} \in \mathbb{R}^4$ is the density of the point object’s two-dimensional position and velocity. In other words, if X is the RFS for cell c , then X can be either \mathbf{x} or \emptyset , and its FISST density is given by

$$\pi_c(X) = \begin{cases} 1 - r & \text{if } X = \emptyset \\ r \cdot p(\mathbf{x}) & \text{if } X = \{\mathbf{x}\} \end{cases} \quad (1)$$

In this application, r is the occupancy probability of cell c with FISST density $\pi_c(X)$. The notion of a grid cell containing a single point object may seem like a crude approximation, especially if grid cells are large enough to contain multiple different real-world objects. However, it is implicitly the same approximation that other occupancy grid approaches make. An object in the real world will, when represented in the map, consist of one or more of these point objects depending on its spatial extent and the grid discretization.

The PHD/MIB filter for the dynamic occupancy map is realized by a set of weighted particles to model $p(\mathbf{x})$. The occupancy probability of a given cell can be easily recovered: it is simply the sum of weights of the particles associated with that cell’s point object.

2.2. Measurement Models

Just as there are two possible truth states for each grid cell (empty and occupied), so too are there two possible information-yielding sensor measurements for each grid cell: “detection” and “miss.” Sensors for probabilistic occupancy mapping may be modeled as beams that extend from the sensor until they hit a solid object in their field of view. This model closely mirrors reality for common sensors like radar, lidar, and stereo cameras. A detection occurs for the cell in which the sensor returns a range less than its maximum range; a miss occurs for all cells in between that cell and the sensor, along the radial direction.

This binary measurement model can be challenging to wield in the presence of sensor pose and measurement uncertainty—how can one be certain that a detection falls in a given cell versus the one adjacent? For this reason, this paper implements a Monte Carlo beam measurement model in which each measurement beam is represented by a set of beams randomly sampled from a distribution that takes

pose and measurement uncertainty into account. Thus, the measurements at epoch k take the form of two arrays: one containing the expected number of detections in each cell, and the other containing the expected number of misses.

Nuss et al. model measurements in each grid cell as an independent Bernoulli observation process, in which each grid cell either has one observation or no observation. However, when pose and sensor uncertainty is non-negligible, as it is in many applications, it is likely that a grid cell will have multiple conflicting observations. In this sense, repeated Bernoulli experiments for a given grid cell at a given point in time are better modeled as a Binomial random variable. Because the chief interest is in estimating r , the occupancy probability of the cell, the natural choice is to model it using a Beta distribution.

$$r \sim f(\rho; \alpha, \beta) = \frac{\rho^{\alpha-1}(1-\rho)^{\beta-1}}{B(\alpha, \beta)} \quad (2)$$

$$\mathbb{E}[r] = \frac{\alpha}{\alpha + \beta} \quad \text{Var}[r] = \frac{\alpha\beta}{(\alpha + \beta)^2(\alpha + \beta + 1)} \quad (3)$$

This model has numerous benefits. It is fully parameterized by two numbers, α and β , and it can be used to compute the variance of the occupancy probability estimate, yielding more information without a much greater computational burden. In general, Bayes theorem for this problem can be written as

$$g(r|Z_1, \dots, Z_n) = \frac{g(r) \prod_{i=1}^n h(z_i|r)}{\int_{\Omega} g(r) \prod_{i=1}^n h(z_i|r) dr} \quad (4)$$

In this expression, $g(r)$ is the Bayesian prior and $\prod_{i=1}^n h(z_i|r)$ is the likelihood; it yields the posterior distribution $g(r|Z_1, \dots, Z_n)$. The integral in the denominator of Equation 4 must be computed numerically. However, as the Beta distribution is a member of the exponential family of distributions, a Beta prior yields a Beta posterior if Bernoulli sampling is used [22, Ch. 13]. More specifically, for a prior distributed as $\text{Beta}(\alpha, \beta)$, the posterior after Bernoulli sampling with k “successes” and m “failures” is distributed as $\text{Beta}(\alpha + k, \beta + m)$. A reasonable choice for a prior to start with for each cell is the $\text{Beta}(1, 1)$ distribution: the uniform distribution on $[0, 1]$. Note that the expected value of $\text{Beta}(1, 1)$ is $\frac{1}{2}$, the typical starting point of a cell’s occupancy probability in a Bayesian occupancy filter in the absence of prior information.

It should also be noted that the Bernoulli random variable modeling the occupancy of the cell is not the same as the Bernoulli random variable modeling the detections and misses from that cell. Different sensors have different properties; a detection in a cell from one sensor may be more likely than one from another. It is reasonable, however, to assume that the two are related. This paper suggests defining pseudo-detections and pseudo-misses as functions of the expected sensor detections and misses. Given a Beta-distributed prior for occupancy probability, $f(\rho; \alpha, \beta)$, one can assume that the posterior takes the form $f(\rho; \alpha + \Delta\alpha, \beta + \Delta\beta)$. One can think of $\Delta\alpha$ as the number of pseudo-detections and $\Delta\beta$ the number of pseudo-misses. A reasonable assumption is that $\Delta\alpha$ and $\Delta\beta$ are functions of the detections and actual misses, respectively. Moreover, one is interested in fusing the detections and misses from heterogeneous sensors. This paper models the pseudo-detections as linear combinations of actual expected detections; that is,

$$\Delta\alpha = \sum_{s=1}^S w_s^{\text{det}} n_s^{\text{det}} \quad \Delta\beta = \sum_{s=1}^S w_s^{\text{miss}} n_s^{\text{miss}} \quad (5)$$

over an index set of sensors S , where w_s^{det} (w_s^{miss}) is the weight associated with detections (misses) from sensor s and n_s^{det} (n_s^{miss}) is the expected number of detections (misses) from that sensor. The weights w_s^{det} and w_s^{miss} may be determined heuristically; one suggestion is to compute them using the update equations for a single measurement in a binary Bayes filter framework. Given the occupancy likelihood functions for cell c and sensor s $g_s^{(c)}(z|o)$ and $g_s^{(c)}(z|\bar{o})$ from Nuss et al. [20], where o denotes the event a cell is occupied and \bar{o} the event that it is empty, it is possible to derive the following expressions for the weights for small α , β :

$$w_s^{\text{det}} \approx \left(\frac{g_s^{(c)}(z = \text{det}|o)}{g_s^{(c)}(z = \text{det}|\bar{o})} - 1 \right) \alpha \quad (6)$$

$$w_s^{\text{miss}} \approx \left(\frac{g_s^{(c)}(z = \text{miss}|\bar{o})}{g_s^{(c)}(z = \text{miss}|o)} - 1 \right) \beta \quad (7)$$

The ratios in these expressions are recognizable as likelihood ratios.

2.3. Risk Evaluation

Risk is a measure of expected loss. The expectation, in this case, is taken over the probability that the ego vehicle will collide with with the point object in cell c over the time interval τ_k . Maintaining the assumption that cells are statistically independent, the risk R_k to which the ego vehicle is exposed at time k can be written as

$$R_k = \sum_c r(c, k) \cdot p_{\text{ego}}(c, k) \cdot L(\mathbf{x}_{\text{ego}}(k), \mathbf{x}_c(k)) \quad (8)$$

where c is the cell index, $r(c, k)$ is the probability that cell c is occupied at epoch k , $p_{\text{ego}}(c, k)$ is the probability that the ego vehicle is in cell c at time k , and $L(\mathbf{x}_{\text{ego}}, \mathbf{x}_c)$ is the loss as a function of the ego vehicle state \mathbf{x}_{ego} and the cell state \mathbf{x}_c . Both \mathbf{x}_{ego} and \mathbf{x}_c are random vectors in \mathbb{R}^4 with two-dimensional position and velocity distributions.

2.4. Loss Function

Understandably, the resulting risk estimate is driven by the choice of loss function. This paper proposes a simple loss function based on kinetic energy, where the loss due to collision in a given cell c is written as

$$L(\mathbf{x}_{\text{ego}}(k), \mathbf{x}_c(k)) = C_1 \|\mathbf{v}_{\text{ego}} - \bar{\mathbf{v}}_c\|^2 + C_2 \mathbb{E}[\|\mathbf{v}_c - \bar{\mathbf{v}}_c\|^2] \quad (9)$$

where \mathbf{v}_{ego} is the expected velocity of the ego vehicle and $\bar{\mathbf{v}}_c$ is the weighted mean of particle velocities in cell c . In the second term, \mathbf{v}_c is the random variable of cell c 's velocity, part of \mathbf{x}_c . The constants C_1 and C_2 are yet another design choice; in the "kinetic energy" case, $C_1 = m_{\text{ego}}m_c/(2(m_{\text{ego}} + m_c))$ and $C_2 = m_c/2$ where m_{ego} is the mass of the ego vehicle in the relevant cell and m_c is the mass of the cell. The cell loss must be normalized by multiplying by the cell area A_c and the time discretization interval τ , ensuring that the risk metric is not sensitive to the choice of discretization.

3. EXPERIMENTAL RESULTS

3.1. Data Capture

In order to demonstrate the benefits of collaborative sensing, the two University of Texas *Sensorium* sensor platforms (Fig. 1) were deployed at an intersection in downtown Austin, Texas (Fig. 2). The



Fig. 1: The University of Texas *Sensorium* is a platform for automated and connected vehicle perception research. It includes stereo visible light cameras, an industrial grade IMU, one to three automotive radar units, a dual-antenna, dual-frequency software-defined GNSS receiver, 4G cellular connectivity, and a powerful internal computer.

data capture was timed such that a bus obscured much of the intersection from the point of view of the vehicle traveling east to west, the ego vehicle. Meanwhile, a collaborator vehicle, traveling in the other direction but turning right (south), had a largely unobstructed view of the entire intersection. Two separate risk evaluations were performed for the ego vehicle: one in which the ego vehicle only has access to its own sensing, and another in which the ego vehicle may also take advantage of sensor information from the collaborator vehicle.

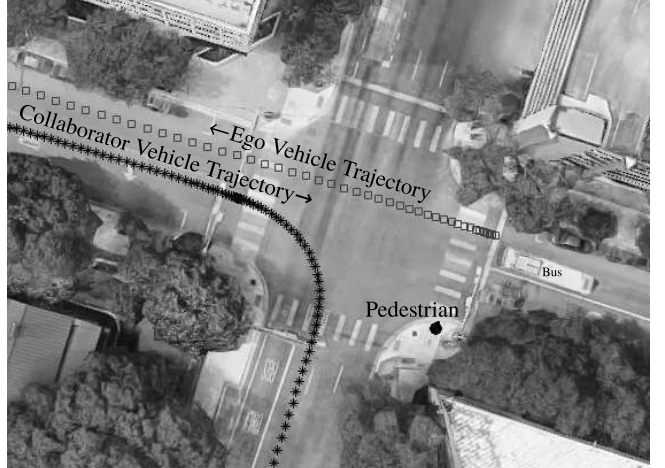


Fig. 2: Illustration of the 8th and Guadalupe Scenario.

Centimeter-accurate vehicle poses were computed based on a dual-antenna RTK receiver with MEMS-grade inertial aiding fused in a loosely-coupled sense in an unscented Kalman filter. The sensor measurement used in this work is depth computed from dense stereo disparity maps and projected into a shared local East, North, Up (ENU) coordinate frame.

Figs. 3 and 4 display the dynamic probabilistic occupancy maps at one time instant using ego-only data and combined ego-collaborator data, respectively. Dark-colored cells are more likely to be occupied, while a light-colored cells are more likely to be empty. Fig. 5 compares the collision risk of the ego vehicle evaluated using these dynamic probabilistic occupancy maps.

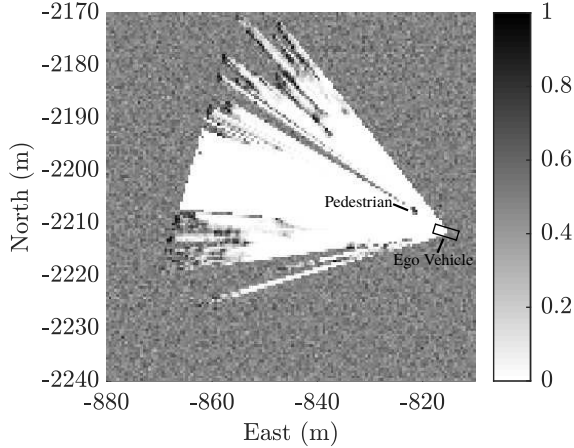


Fig. 3: Occupancy map at $t = 61.6$ seconds with data from only the ego vehicle.

3.2. Discussion

Collaborative sensing allows the ego vehicle to effectively see beyond the field of view of its own sensors. In the presented scenario, collaborative sensing enables the ego vehicle to see the pedestrian cross the street while it is obscured by the bus. In addition, collaborative sensing allows the vehicle to more confidently rule out the possibility that there are other objects out of its field of view that pose a risk for collision.

The initial increase in the accumulated risk is due to the ego vehicle sharing its immediate environment with other nearby objects, and its increase in velocity as it accelerates into the intersection. Once in the intersection, however, the ego vehicle is able to combine its sensing with the collaborator vehicle’s sensing to verify that the intersection is indeed clear, and the accumulated risk curve flattens. As the vehicle exits the map, the risk increases again as the boundaries of the map are restricted to the “ignorant” Beta(1, 1) prior.

It is clear that the benefit of sensor sharing is reduced collision risk from Fig. 5. It is also worth noting that the collaborative risk estimate is also more confident, as can be inferred from the $+2\sigma$ line. In this case, of course, there was no collision; this estimate of collision risk also takes into account exposure to potential collisions due to objects in unobserved regions of the environment. In a situation where collaborative sensing actually increases the expected collision risk (for example, by warning the ego vehicle about an impending unpredicted collision), the variance of the collision risk estimate should decrease thanks to the increased certainty provided by collaborative sensing.

4. CONCLUSIONS

This paper presents a framework for automotive collision risk estimation based on a Bayesian occupancy filter augmented with a collision loss function. To test the framework, a data capture was conducted at an intersection in downtown Austin, Texas. The results of the experiment support the notion that cooperative sensing can reduce exposure to collision risk.

This risk framework can estimate collision risk for a known trajectory, as presented in this paper; alternatively, it can be used for motion planning by computing the least risky trajectory given cur-

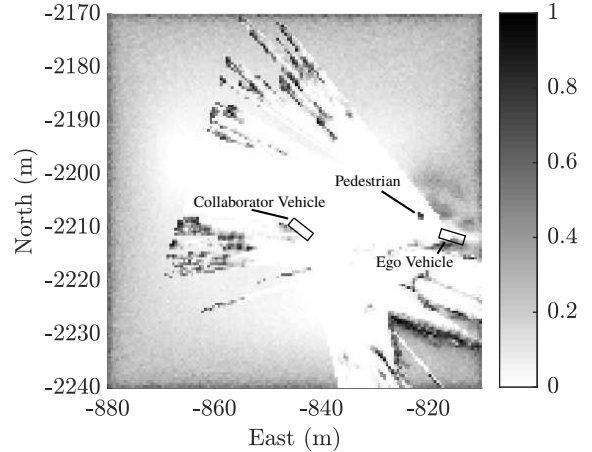


Fig. 4: Occupancy map at $t = 61.6$ seconds built with data from both vehicles.

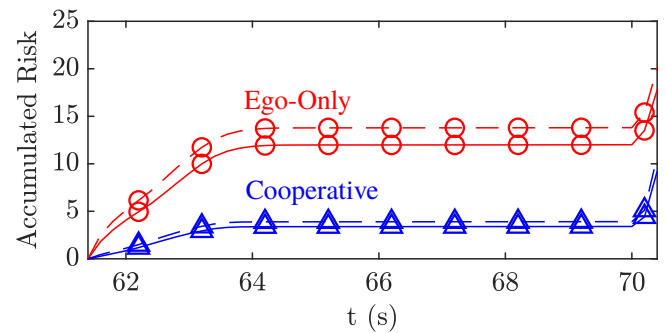


Fig. 5: Accumulated risk profiles for the ego vehicle. The solid lines represent expected accumulated risk, while the dashed lines represent the expected accumulated risk plus two standard deviations.

rent sensing. The use of cooperative sensing raises additional questions: if communication bandwidth is limited, which sensor data is the most useful? In this way, the motion planning problem can be reframed in terms of active sensing and data exchange.

5. ACKNOWLEDGMENTS

This work has been supported by Honda R&D Americas, Inc. as an affiliate of The University of Texas Situation-Aware Vehicular Engineering Systems (SAVES) Center (<http://utsaves.org/>), an initiative of the Wireless Networking and Communications Group.

6. REFERENCES

- [1] Shai Shalev-Shwartz, Shaked Shammah, and Amnon Shashua, “On a formal model of safe and scalable self-driving cars,” *arXiv preprint arXiv:1708.06374*, 2017.
- [2] Tyler GR Reid, Sarah E Houts, Robert Cammarata, Graham Mills, Siddharth Agarwal, Ankit Vora, and Gaurav Pandey, “Localization requirements for autonomous vehicles,” *arXiv preprint arXiv:1906.01061*, 2019.
- [3] Yicong Wang, Gustavo de Veciana, Takayuki Shimizu, and Hongsheng Lu, “Performance and scaling of collaborative

- sensing and networking for automated driving applications,” in *2018 IEEE International Conference on Communications Workshops (ICC Workshops)*. IEEE, 2018, pp. 1–6.
- [4] Adrian Broadhurst, Simon Baker, and Takeo Kanade, “Monte Carlo road safety reasoning,” in *IEEE Proceedings. Intelligent Vehicles Symposium, 2005*. IEEE, 2005, pp. 319–324.
- [5] Matthias Althoff, Olaf Stursberg, and Martin Buss, “Model-based probabilistic collision detection in autonomous driving,” *IEEE Transactions on Intelligent Transportation Systems*, vol. 10, no. 2, pp. 299–310, 2009.
- [6] Stéphanie Lefèvre, Dizan Vasquez, and Christian Laugier, “A survey on motion prediction and risk assessment for intelligent vehicles,” *ROBOMECH journal*, vol. 1, no. 1, pp. 1, 2014.
- [7] Ashwin Carvalho, Stéphanie Lefèvre, Georg Schildbach, Jason Kong, and Francesco Borrelli, “Automated driving: The role of forecasts and uncertainty—A control perspective,” *European Journal of Control*, vol. 24, pp. 14–32, 2015.
- [8] Stefan Hoermann, Felix Kunz, Dominik Nuss, Stephan Reuter, and Klaus Dietmayer, “Entering crossroads with blind corners. A safe strategy for autonomous vehicles,” in *2017 IEEE Intelligent Vehicles Symposium (IV)*. IEEE, 2017, pp. 727–732.
- [9] S. Hoermann, P. Henzler, M. Bach, and K. Dietmayer, “Object detection on dynamic occupancy grid maps using deep learning and automatic label generation,” in *2018 IEEE Intelligent Vehicles Symposium (IV)*, June 2018, pp. 826–833.
- [10] Sebastian Thrun, Wolfram Burgard, and Dieter Fox, *Probabilistic robotics*, MIT press, 2005.
- [11] Marcelo Saval-Calvo, Luis Medina-Valdés, José Castillo-Secilla, Sergio Cuenca-Asensi, Antonio Martínez-Álvarez, and Jorge Villagrà, “A review of the Bayesian occupancy filter,” *Sensors*, vol. 17, no. 2, pp. 344, 2017.
- [12] Christophe Coué, Cédric Pradalier, Christian Laugier, Thierry Fraichard, and Pierre Bessière, “Bayesian occupancy filtering for multitarget tracking: an automotive application,” *The International Journal of Robotics Research*, vol. 25, no. 1, pp. 19–30, 2006.
- [13] Mathias Perrollaz, John-David Yoder, Amaury Nègre, Anne Spalanzani, and Christian Laugier, “A visibility-based approach for occupancy grid computation in disparity space,” *IEEE Transactions on Intelligent Transportation Systems*, vol. 13, no. 3, pp. 1383–1393, 2012.
- [14] Tobias Gindele, Sebastian Brechtel, Joachim Schroder, and Rudiger Dillmann, “Bayesian occupancy grid filter for dynamic environments using prior map knowledge,” in *2009 IEEE Intelligent Vehicles Symposium*. IEEE, 2009, pp. 669–676.
- [15] Hongqi Fan, Tomasz Piotr Kucner, Martin Magnusson, Tiancheng Li, and Achim J Lilienthal, “A dual PHD filter for effective occupancy filtering in a highly dynamic environment,” *IEEE Transactions on Intelligent Transportation Systems*, vol. 19, no. 9, pp. 2977–2993, 2017.
- [16] Radu Danescu, Florin Oniga, and Sergiu Nedevschi, “Modeling and tracking the driving environment with a particle-based occupancy grid,” *IEEE Transactions on Intelligent Transportation Systems*, vol. 12, no. 4, pp. 1331–1342, 2011.
- [17] Amaury Nègre, Lukas Rummelhard, and Christian Laugier, “Hybrid sampling Bayesian occupancy filter,” in *2014 IEEE Intelligent Vehicles Symposium Proceedings*. IEEE, 2014, pp. 1307–1312.
- [18] Lukas Rummelhard, Amaury Nègre, and Christian Laugier, “Conditional Monte Carlo dense occupancy tracker,” in *2015 IEEE 18th International Conference on Intelligent Transportation Systems*. IEEE, 2015, pp. 2485–2490.
- [19] Sascha Steyer, Christian Lenk, Dominik Kellner, Georg Tanzmeister, and Dirk Wollherr, “Grid-based object tracking with nonlinear dynamic state and shape estimation,” *IEEE Transactions on Intelligent Transportation Systems*, 2019.
- [20] Dominik Nuss, Stephan Reuter, Markus Thom, Ting Yuan, Gunther Krehl, Michael Maile, Axel Gern, and Klaus Dietmayer, “A random finite set approach for dynamic occupancy grid maps with real-time application,” *The International Journal of Robotics Research*, vol. 37, no. 8, pp. 841–866, 2018.
- [21] Ba-Tuong Vo and Ba-Ngu Vo, “Labeled random finite sets and multi-object conjugate priors,” *IEEE Transactions on Signal Processing*, vol. 61, no. 13, pp. 3460–3475, 2013.
- [22] Arjun K Gupta and Saralees Nadarajah, *Handbook of beta distribution and its applications*, CRC press, 2004.